ACCOUNTS
of chemical research

Nanographene and Graphene Edges: Electronic Structure and Nanofabrication

SHINTARO FUJII* AND TOSHIAKI ENOKI*

Department of Chemistry, Tokyo Institute of Technology, 2-12-1 Ookayama, Meguro-ku, Tokyo 152-8551, Japan

RECEIVED ON MAY 19, 2012

CONSPECTUS

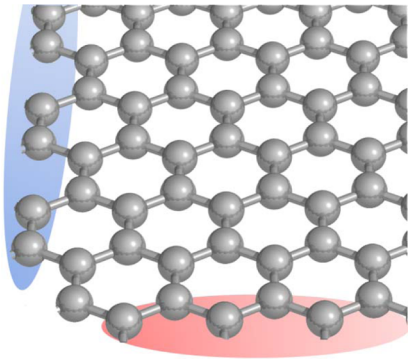

Graphene can be referred to as an infinite polycyclic aromatic hydrocarbon (PAH) consisting of an infinite number of benzene rings fused together. However, at the nanoscale, nanographene's properties lie in between those of bulk graphene and large PAH molecules, and its electronic properties depend on the influence of the edges, which disrupt the infinite π-electron system. The resulting modulation of the electronic states depends on whether the nanographene edge is the armchair or zigzag type, corresponding to the two fundamental crystal axes. In this Account, we report the results of fabricating both types of edges in the nanographene system and characterizing their electronic properties using a scanning probe microscope.

We first introduce the theoretical background to understand the two types of finite size effects on the electronic states of nanographene (i) the standing wave state and (ii) the edge state which correspond to the armchair and zigzag edges, respectively. Most importantly, characterizing the standing wave and edge states could play a crucial role in understanding the chemical reactivity, thermodynamic stability and magnetism of nanosized graphene—important knowledge in the design and realization of promising functionalized nanocarbon materials.

In the second part, we present scanning probe microscopic characterization of both edge types to experimentally characterize the two electronic states. As predicted, we find the armchair-edged nanographene to have an energetically stable electronic pattern. The zigzag-edged nanographene shows a nonbonding (π radical) pattern, which is the source of the material's electronic and magnetic properties and its chemical activity. Precise control of the edge geometry is a practical requirement to control the electronic structure. We show that we can fabricate the energetically unstable zigzag edges using scanning probe manipulation techniques, and we discuss challenges in using these techniques for that purpose.

1. Introduction

Since its successful isolation in 2004,[1] graphene has attracted intensive experimental research interest in physics, mostly due to its unique electronic properties, such as the anomalous quantum Hall effect[2] and Klein tunneling,[3] which are a consequence of massless Dirac fermions with linear energy dispersion near the Fermi level.[4] From a chemical perspective, graphene can be referred to as an infinite polycyclic aromatic hydrocarbon (PAH) that consists of an infinite number of benzene rings fused together. As the size of graphene becomes gradually smaller, the electronic properties can be described in terms of organic chemistry electronic theory.[5] Our particular interest is nanosized graphene (nanographene), which is ca. 1−10 nm[6] and is in-between small PAH molecules and graphene. On this scale, richer nanosize effects on the electronic properties are expected due to the richer boundary conditions, which can be understood using different approaches from chemistry and solid state physics. There have been extensive reports on the electronic properties of nanosized graphene materials in the interdisciplinary regions of chemistry and physics.[6−12] In this Account, we attempt to provide an understanding of the electronic properties of nanographene, which have not been well-characterized to date, possibly due to the ill-defined structure and the difficulty of synthesis due to its lower solubility.

We first introduce the theoretical background to understand the two types of finite size effects on the electronic

Published on the Web 11/21/2012 www.pubs.acs.org/accounts
10.1021/ar300120y

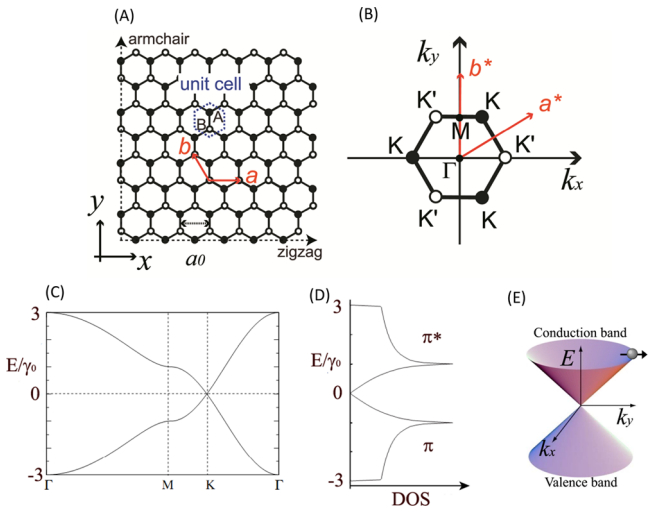

FIGURE 1. (A) Graphene honeycomb bipartite lattice structure in real space, where the black and white circles denote A- and B-sublattice sites, respectively, a_0 is the lattice constant and $\mathbf{a} = (a, 0)$ and $\mathbf{b} = (-a/2, \sqrt{3}a/2)$ are the primitive vectors. The unit cell is indicated by a dotted hexagon. (B) First BZ of graphene. Reciprocal lattice vectors are denoted by $\mathbf{a}^*$ and $\mathbf{b}^*$. $\mathbf{K} = 2\pi/a(1/3, 1/\sqrt{3})$, $\mathbf{K}' = 2\pi/a(2/3, 0)$, $\Gamma = (0, 0)$. (C) π-band structure of graphene along Γ-M-K-Γ within the irreducible BZ. γ_0 is the transfer integral between nearest-neighbor carbon sites ($\gamma_0 = 3.16$ eV). (D) Density of states (DOS) of the π band. (E) Three dimensional π-band structure of graphene near the *K* point. Pseudospin is indicated by an arrow.

states of nanographene: (i) the standing wave state[13−16] and (ii) the edge state,[17−23] which are alternatively switched back and forth depending on the two distinct edge types (i.e., armchair and zigzag edges). Most importantly, clarification of the standing wave state and edge state could play a crucial role in understanding the presence and absence of chemical reactivity, thermodynamic stability and magnetism for nanosized graphene. Thus, improved understanding of the electronic states is necessary to design and realize promising functionalization of nanocarbon materials. In the second part, we present scanning tunneling microscopic (STM) characterization to experimentally determine the two electronic states and provide experimental evidence.[13−16,19−21] Challenges to tailor nanographene into specific size and edge-shape using the scanning probe manipulation technique[24] are also discussed. Thus, precise control of the edge geometry is a practical requirement to control the electronic structure.

2. Electronic Structure of Graphene

A carbon atom has a total of six electrons that occupy the atomic orbitals as $1s^2\ 2s^2\ 2p^2$. The 1s electrons in the inner K-shell are essentially inert and do not contribute to chemical bonding. In valence bond theory, when carbon atoms are arranged in a honeycomb lattice, the 2s, $2p_x$, and $2p_y$ orbitals hybridize to form three planar sp^2 orbitals, which are responsible for the formation of strong σ bonds between the neighboring atoms in the graphene lattice. The remaining $2p_z$ orbitals perpendicular to the graphene plane form π bonds and are delocalized, which determines its electronic, magnetic and chemical properties.

Figure 1A and B shows the lattice structure and the first Brillouin zone (BZ) of graphene, respectively. Graphene has a honeycomb bipartite lattice structure with a hexagonal unit cell containing two independent A and B sublattice sites. This unit cell in the real space is transcribed to the first BZ with two independent high-symmetry points at its corners (K or K′ points), which are associated with the lattice degree of freedom of 2 (A and B atoms in the unit cell). In a simple tight-binding (TB) description for the graphene π bands,[25] the electronic state is represented by a linear superposition of π states belonging to the A and B atoms. Following this scheme, the electronic energy dispersion and the density of states (DOS) can be described as shown in Figure 1C and D, respectively,[25,26] by considering nearest-neighbor interaction for the $2p_z$ orbitals, but by neglecting the overlap between wave functions centered at different atoms. The cone-shaped conduction and valence π bands (Figure 1E), which have linear k-dependence near the K and K′ points, touch each other at a point called the Dirac point, at which the Fermi level is located. Therefore, graphene can be called a zero-gap semiconductor and its electronic properties are mostly determined by the π states near the K and K′ points. The TB model thus obtained is effectively understood on the basis of massless Dirac fermions (Weyl equation) in a relativistic quantum system with momentum *p*, as given by the following low-energy effective Hamiltonian:

$$\hat{H} = \sigma v_F p \qquad (1)$$

where v_F is the Fermi velocity ($v_F = 3\gamma_0 a_{cc}/2\hbar \approx (1/300c)$; γ_0 is the intrasheet transfer integral, *c* is the speed of light, $a_{cc} = 0.142$ nm is the intrasheet C−C bond length, and σ is the Pauli matrix of a spin, known as the pseudospin, which is effectively converted from the lattice degree of freedom of 2. This suggests that graphene becomes magnetic with localized spins if the symmetry between sublattices A and B is broken, which typically appears at the edges when a graphene sheet is cut into fragments.

Next, let us examine the electronic properties (states) of π electrons in graphene with respect to resonance theory. To begin, Clar theory[5] is introduced to treat large numbers of

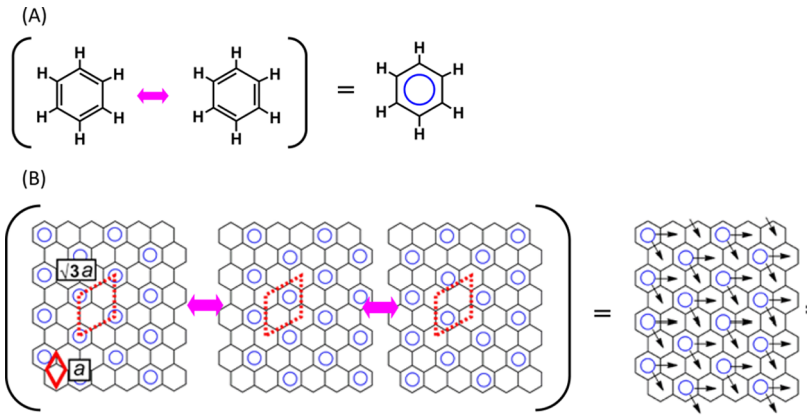

FIGURE 2. Resonance structures of (A) benzene and (B) graphene, in which the unit cells of graphene and the Clar sextets are indicated by solid (*a*) and dotted lines ($\sqrt{3}a$), respectively. Sextet migration is indicated by an arrow attached to the sextet (blue circle).

possible resonance structures with increasing system size. Benzene, the smallest building block of graphene, can be represented by the resonance or superposition of two complementary Kekulé configurations. The six delocalized π electrons are depicted by a circle called a sextet in Clar theory (Figure 2A). The delocalized character in a sextet can be understood by the diamagnetic response of benzene, as with graphene. According to Clar's rule for a given geometry of fused benzene rings, the representation with the maximum number of Clar sextets is the most representative formula, which has proven to be an intuitive yet adequate model for π electron distributions of small PAH molecules.[27,28] This is because a Clar formula with *n* Clar sextets represents the resonance of 2^n Kekulé formulas, and therefore, maximizing the number of Clar sextets is equivalent to maximizing the number of resonant Kekulé formulas in one Clar representation.[5,28] Based on this rule, the valence bond configuration of graphene can be depicted by the resonance of three Clar formulas having a $\sqrt{3}a \times \sqrt{3}a$ superlattice (Figure 2B). As a result, all electrons are distributed uniformly over the network without bond alternations. Note that all electrons belong to Clar sextets and no localized double bonds are present. Such a structure is referred to as fully benzenoid for small PAH molecules and is indicative of particularly higher thermodynamic stability and lower chemical reactivity.[5] In the following section, we will introduce the modulation of the electronic properties of the infinite π electron system with the presence of edges and its dependence on the edge type.

3. Standing Wave State for Armchair Edge

To understand the formation of standing wave states,[14,15] let us consider a scattering event of electron waves at graphene edges. In this model, plane waves with a wavelength

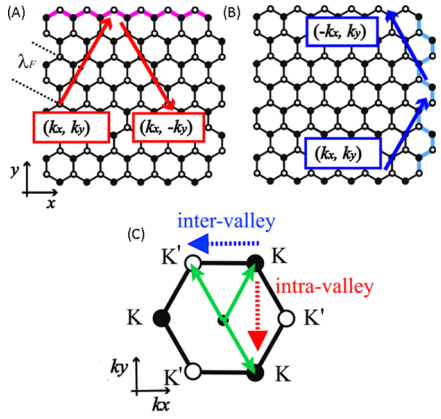

FIGURE 3. Electron wave scattering events at (A) zigzag and (B) armchair edges. Edge boundaries are represented by red and blue lines for (A) zigzag and (B) armchair edges, respectively. λ_F is the Fermi wavelength ($3a/2$). Electron wave with wavevector components $\boldsymbol{k_{in}}$ (k_x, k_y) is elastically scattered at the edges, which leads to a change in the wavevector as indicated by $\boldsymbol{k_Z}$ (k_x, $-k_y$) and $\boldsymbol{k_A}$ ($-k_x$, k_y) at the zigzag and armchair edges, respectively. (C) Corresponding transitions of the wavevector in reciprocal space due to intravalley and intervalley scatterings at zigzag and armchair edges, respectively.

of λ_F ($3a/2$) propagate into space along zigzag directions, which are uniquely determined by wavevectors at the K (K′) points. Figure 3A and B shows that the π state electron in the K (K′) valley is elastically scattered at zigzag or armchair edges, respectively. From the momentum conservation along the edges, scattering at the zigzag edges leads to a change in the *y*-component of the wavevector. This corresponds to a K → K (K′ → K′) (intravalley) transition in the momentum space, as represented by the red arrow in Figure 3C. In contrast, scattering at an armchair edge leads to a change in the x-component of the wavevector and this corresponds to a K → K′ (K′ → K) (intervalley) transition, as represented by the blue arrow in Figure 3C. The transitions between the two nonequivalent states at K and K′ cause mixing of the two

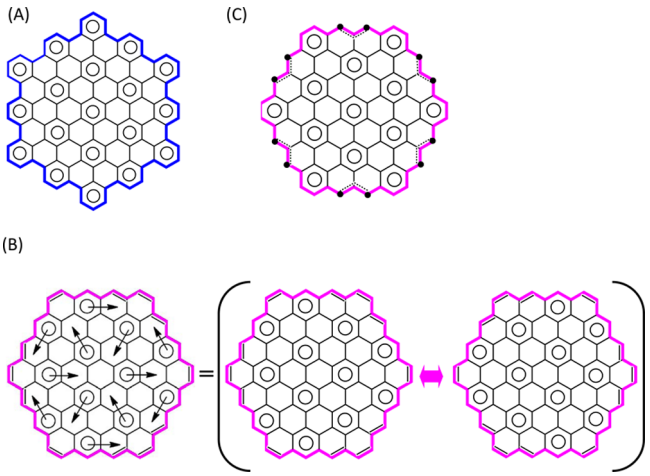

FIGURE 4. Clar formulas of (A) armchair-terminated nanographene ($C_{114}H_{30}$) and (B,C) zigzag-terminated nanographene ($C_{96}H_{24}$), where edges are represented by bold lines. The resonance hybrid in (B) with sextet migrations indicated by an arrow attached to the sextet (circle) can be decomposed into two Clar formulas. Resonance between C═C−C* and C*−C═C configurations is represented by dotted double bonds in (C).

wave functions with K′ and K, and accordingly an electron wave interference occurs with the scattering event.[13,29,30]

The origin of the π states caused by the intervalley transition at the armchair edge can be understood from a different aspect in resonance theory, or conventional valence bond theory. For example, the resonance hybrid of benzene can be represented by the two resonant Kekulé structures (Figure 2A). In a crude discussion, the hybrid valence π state of a PAH molecule may be described as a superposition of possible resonant states (i.e., interacting Kekulé structures). The increasing number of possible resonant structures in this model leads to energetic stabilization of the hybrid state due to an increase in coupling or interaction of the system.[28] This is referred to as resonance stabilization, which can be explained by the delocalization of π electrons in a sextet rather than an increase in possible resonance structures. The Clar formula represents the resonant Kekulé structure with the largest degree of freedom, and thus with higher energy stabilization. Here, we consider π electron arrangements in typical Clar formulas for nanographene with zigzag or armchair terminations (Figure 4). Figure 4A shows the Clar formula for armchair-terminated nanographene ($C_{114}H_{30}$), which is represented by one unique structure consisting of 19 sextets without localized double bonds. Therefore, this is classified as a fully benzenoid molecule with lower chemical reactivity according to Clar theory. This localization of the sextet is indicative of the standing wave state due to intervalley scattering and interference of electron waves near the armchair edge.

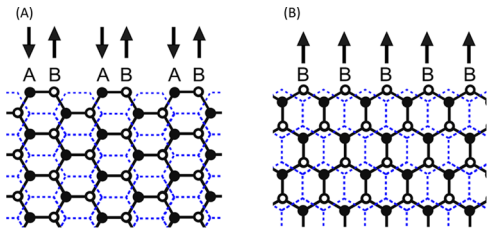

FIGURE 5. Schematic illustrations of the sublattice symmetry of (A) armchair and (B) zigzag edges. The up- and down-arrows represent pseudospins. A dotted hexagon indicates the paring of A and B atoms.

On the other hand, zigzag-terminated nanographene has a nonunique Clar structure, as shown in Figure 4B and C, and therefore, clear localization of sextets is not expected, but can be explained by the absence of electron wave interference at the bulk zigzag edge due to intravalley scattering.

4. Edge State for Zigzag Edge

The presence of the edge states at zigzag graphene edges was originally predicted by TB analysis of graphene nanoribbons,[17,18] in which a zigzag-terminated nanoribbon shows a peculiar sharp DOS peak at the Fermi level that arises from the partly flat bands, whose wave functions are mainly localized on the zigzag edge. (Figure S1, Supporting Information). The origin of the edge state can be intuitively understood in terms of the symmetry of the pseudospin of the Dirac fermions in the bipartite lattice. The zigzag edge is terminated by only one of the A or B sublattices, while the armchair edges are always terminated by paired A and B atoms in the sublattices, as illustrated in Figure 5. Accordingly, the symmetry of the pseudospin is broken in the zigzag edge, which produces the edge state. The sharp discontinuity in the graphene lattice, accompanied by the broken symmetry between sublattices A and B at the zigzag edge, induces a gauge field, so that the edge state is strongly spin polarized. Accordingly, such localized edge states give rise to modulated spin magnetism in addition to the diamagnetic properties associated with the cyclotron motion of the itinerant electrons in graphene. The edge state is capable of generating spin ordering due to electron−electron interaction. For example, ferromagnetic ordering along the zigzag edge and the mutual antiparallel orientation of the magnetic moments localized at opposite edges in a zigzag-graphene nanoribbon have been predicted using a simple Hubbard model,[17,18] in which an on-site Coulomb potential ($U/\gamma_0 =$ 0.1, γ_0 = transfer integral) is introduced in the nearest-neighbor TB Hamiltonian. Here the edge-state spins localized in the zigzag edges have a feature of weakly anisotropic Heisenberg system due to a small spin−orbit interaction of carbon atoms.[31]

The edge state at the zigzag edge can be found in the electronic structure of giant PAH molecules. There have been previous theoretical attempts to investigate the edge shape-dependent electronic properties of PAH molecules within the Hückel or TB approximations, in which the amplitudes of the HOMO are almost uniformly distributed in the entire region for an armchair-terminated PAH consisting of several hundred carbon atoms, whereas the HOMO of the zigzag-terminated PAH possesses the largest amplitude at the edge.[32−34] The larger amplitude of the MO, that is, the radical character, at the edge can be understood from its Clar formula. Although Clar theory was originally developed for the representation of Kekulé molecules without unpaired electrons,[5] Clar structures of zigzag-terminated nanographene can be constructed, as shown in Figure 4B and C. In contrast to the Clar formula of armchair-terminated nanographene (Figure 4A), in which the chemical structure is represented by a unique Clar structure, the Clar formulas of zigzag-terminated nanographene are nonunique with double bonds or unpaired electrons at the edges. The chemical structure shown in Figure 4B is represented by 12 sextets and 12 double bonds, while an additional sextet can be formed by cleaving 6 double bonds, as shown in Figure 4C, in which 13 sextets exist. From resonance theory, the energetic loss of π bond cleavages can be partially compensated by resonance stabilization due to the formation of an additional aromatic sextet. Thus, the resonance hybrid can be constructed by a superposition of the two states, in which the π states are characterized by the radical nature at the edges with no clear preferential location of the sextets in the honeycomb lattice.

5. STM Observation of the Standing Wave State near the Armchair Edge

In an infinite graphene system, the π states on A and B sites (Figure 1A) have the same amplitude, that is, all π electrons are distributed uniformly in the honeycomb lattice (Figure 2B). Thus, STM images will show a honeycomb pattern with a nearest-neighbor spacing of $a/\sqrt{3}$ (0.14 nm) for bulk graphene, or a hexagonal pattern with a periodicity of a (0.24 nm) for bulk graphene on graphite, due to the interlayer interaction. When an edge is introduced in the bulk, the electronic structure is modulated from that of infinite graphene. Figure 6A and B shows the modulated electronic state in a form of a fine honeycomb pattern near an armchair edge of graphene on graphite observed using low temperature STM under ultrahigh vacuum (UHV).[13] A 3-fold symmetric fine structure is evident in the individual superlattice site. At first

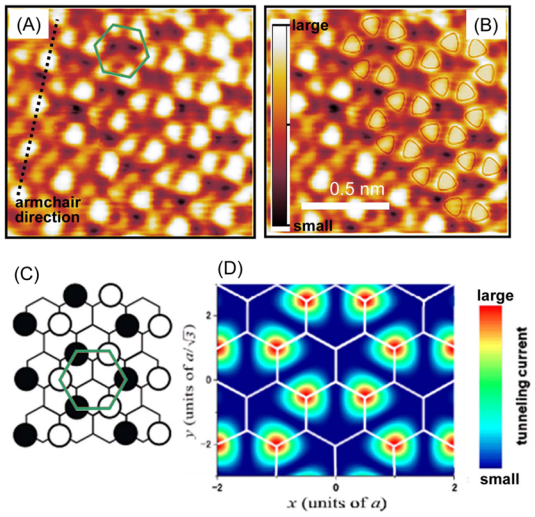

FIGURE 6. (A) Atomic-resolution UHV STM tunneling current image (1.4×1.2 nm^2) taken in the vicinity of an armchair edge, which is approximately 1 nm away from the right edge with a length of several hundred nanometers. The armchair direction is indicated by a dotted line. A honeycomb pattern is indicated by green lines. (B) Overlaid honeycomb pattern on image (A). The sample bias voltage is 20 mV. (C) 2D squared-amplitude mapping of the wave function near the armchair edge. Open and filled circles correspond to + and − phase wave functions, respectively. (D) Calculated 2D current mapping of the honeycomb superlattice pattern and 3-fold symmetry. [after ref 13.] Adapted with permission from ref 13. Copyright 2010 American Physical Society.

glance, there is likely to be no clear relationship between the ideal honeycomb pattern of the graphene lattice ($a/\sqrt{3}$ (0.14 nm)) and the larger honeycomb pattern with a nearest-neighbor distance of $\sqrt{3}a$ (0.42 nm); however, this relationship can be understood using a simple mathematical argument.

As expected from the fully benzenoid aromatic character of armchair-terminated nanographene, the armchair edge is energetically stable. Straight armchair edges with lengths of several hundred nanometers can be readily observed using STM,[13,19] while long zigzag edges are difficult to observe. The armchair edges are straight and sufficiently long to apply a simple boundary condition of wave functions along the edge direction in a TB model. This allows the observed fine structure to be reproduced in detail from a simple derivation of the wave functions. Considering an infinite potential barrier on the armchair edge in the TB scheme, the wave function (ψ_B) on a B atom around the armchair edge is expressed by

$$\Psi_B(R_B) \propto \left(-\exp(\ -iKR_B) + \exp(iK'R_B) \right) \qquad (1)$$

owing to the interference between K and K′ wave functions, where R_B is the translation vector of the B atom sites.[14]

The STM image can be simulated by two-dimensional (2D) squared-amplitude mapping of the wave function (eq 1).

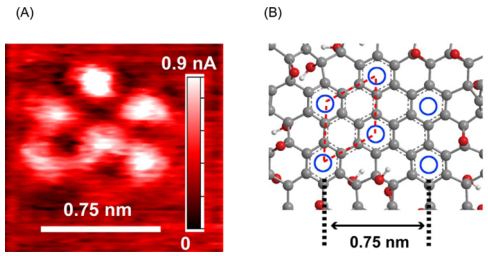

FIGURE 7. Tunneling current image of a nanographene fragment of oxidized graphene on Au(111) at a sample bias voltage of 50 mV. (B) Proposed schematic model (carbon, gray; oxygen, red; hydrogen, white). Dotted red lines indicate the $\sqrt{3}a \times \sqrt{3}a$ pattern with respect to the hexagonal graphene sublattices. Next nearest-neighbor distance of the sextets is ca. 0.75 nm ($3a$, $a = 0.25$ nm). [after ref 16.] Adapted with permission from ref 16. Copyright 2012 Wiley–VCH.

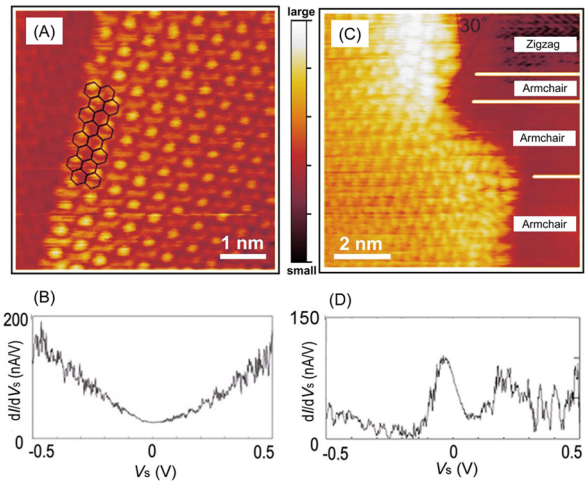

FIGURE 8. (A) Atomically resolved UHV-STM tunneling current image (5.6×5.6 nm^2) of an armchair edge. A model of the honeycomb lattice is superimposed on the image to clarify the edge structures. (B) dI/dV_s curve from STS measurements taken at the edge shown in (A). (C) Atomically resolved STM image of zigzag and armchair edges (9×9 nm^2). (D) dI/dV_s curve from STS data at a zigzag edge in (C). Images were acquired with a sample bias voltage of $V_s = 20$ mV. [after ref 19.] Adapted with permission from ref 19. Copyright 2005 American Physical Society.

The resulting 2D mapping image shown in Figure 6C reproduces the experimentally observed honeycomb patterns. The superperiodic distribution of π states, that is, the localized state decaying into the bulk, is the standing wave state due to intervalley scattering of the electron wave at the armchair edge, or the localization of sextets in armchair-terminated nanographene. This is a typical nanosize effect of the π electronic system and is indicative of lower chemical reactivity and higher energetic stability. Taking into account the phase of the wave function, the formation of the 3-fold symmetry fine structure can be further explained in detail. In the honeycomb superlattice, the signs of the wave functions at adjacent sites are opposite to each other. The antibonding coupling of the wave functions with a node in the middle between the two sites leads to the 3-fold symmetrical fine structure evident in the STM image. This is well-reproduced in the simulated STM[35] image shown in Figure 6D.

Let us discuss another example of electron wave interference. Armchair-terminated nanographene can be represented by a unique Clar formula with $\sqrt{3}a \times \sqrt{3}a$ periodicity of the localized sextets, which indicates the standing wave state. Such a sextet pattern can be identified in the π states of nanographene fragments in oxidized graphene.[16] Nanographene fragments are prepared by oxidizing graphene sheets and are isolated by oxidized sp^3 carbon backbones. Figure 7 shows a tunneling current image of a nanofragment and a proposed schematic model, in which armchairlike edges are formed by oxidation. The armchair edges prohibit sextet migration according to Clar theory (Figures 4A and 7B), and thus, such localized sextets with the $\sqrt{3}a \times \sqrt{3}a$ pattern predicted by the Clar formula[36] can be experimentally confirmed by the π state characterization in the tunneling current image,[16,37] although symmetry of the observed pattern in the small π system is degraded by sample deformation due to the surrounding oxidized sp^3 carbon backbones.

6. STM Characterization of the Edge State

Zigzag edges prepared under ambient atmospheric conditions are usually covered by oxygen-containing functional groups, due to reactions with oxygen.[19] This is a consequence of the higher reactivity of the π radicals at the zigzag edges.[38] Therefore, it has been a challenge to characterize the intrinsic electronic properties of zigzag edges. To overcome this problem, all preparation and measurement procedures should be conducted under UHV conditions to avoid exposure to the atmosphere. The graphene edges are heat-treated at 800 °C in UHV to remove the oxygen-containing functional groups, and then hydrogen terminated by exposure to atomic hydrogen.[19,20] Figure 8 shows typical examples of UHV-STM images and scanning tunneling spectroscopy (STS) spectra of hydrogenated graphene edges.[20] STS spectra (Figure 8B) measured at the armchair-terminated edge region (Figure 8A) indicate an almost linear energy dispersion, similar to that of bulk graphene in the vicinity of the Fermi level.[4] In contrast, the zigzag edge has completely different features from those of the armchair edges. The zigzag edges tend to be defective and short, and are frequently embedded between armchair edges, as shown in Figure 8C, which is due to the energetically unstable structure of the less aromatic zigzag edges.[28,36,39] As discussed in

section 3, the standing wave state is not expected near the zigzag edges, due to the absence of intervalley scattering (Figure 3). Consequently, the zigzag edges in Figure 8C show a typical hexagonal pattern with a periodicity of a (0.24 nm), which is the representative electronic state of bulk graphene on graphite. Apart from the absence of the standing wave state, the most significant feature of zigzag edges is the edge state.[17,18] In clear contrast to the armchair edge (Figure 8B), the STS spectrum for the zigzag edge (Figure 8D) shows a sharp DOS peak at the Fermi level, in addition to the linear dispersion, which is in good agreement with the nearest-neighbor TB prediction.[17,18] The edge state has a strongly localized nature at the zigzag edges, which is evident as brighter spots (i.e., larger LDOS) at the short zigzag edges in the STM image of Figure 8C. Note that the STS profile does not show electron−hole symmetry with respect to the Dirac point ($V_s = 0$ V), in disagreement with the theoretical prediction given in Supporting Information Figure S1C and D. The observed electron−hole asymmetry in the LDOS peak in Figure 8D indicates the presence of a nonzero local potential at the edge. The on-site potential is caused by (i) the potential generated by non-negligible charge transfer at the edges and (ii) the modification of on-site energies of π-orbitals due to local strain effects inevitably present at the edges. In the TB analysis, the inclusion of next nearest-neighbor hopping processes breaks the effective electron−hole symmetry at the edges,[40] which has shown to be analogous to modification of the on-site potential at the edges.[41] It should be noted that there is an interesting relationship between the edge state of graphene edges and the electronic structure of radical addition products, such as those arising from hydrogen chemisorption defects[42,43] and the aryl radical addiction product from diazonium chemistry.[44,45] Radical addition extracts a π electron from a carbon A-atom in bulk graphene, which leads to the formation of a localized unpaired electron on a B-atom. Thus, radical addition breaks the symmetry of the pseudospin and could cause the localized state and magnetism.

7. Fabrication of Zigzag Edges by AFM Manipulation

Graphene or graphite can be oxidized by reaction with strong oxidants to yield graphene oxide or graphite oxide. In most of the graphene oxide, oxidation produces a graphene sheet randomly bonded with oxygen-containing functional groups, which is thus irregularly corrugated. However, among the graphene oxide samples prepared, regularly wrinkled graphene oxide sheets appear, as shown in

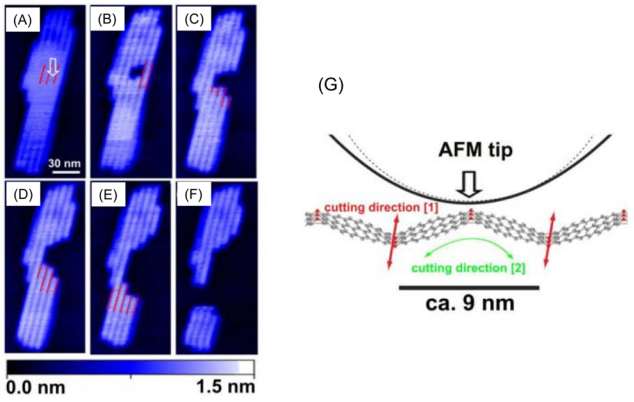

FIGURE 9. Series of noncontact AFM images of a graphene oxide sheet with ordered wrinkles before and after AFM manipulation. The wrinkles are caused by regular arrangement of 1D arrays of epoxy rings running along a zigzag direction introduced by chemical oxidation. (A) Point contact between the sheet and the AFM probe is made at the center of the sheet. The white arrow indicates the contact area. The region indicated by the red lines is removed after the point contact. (B−F) The sheet begins to spontaneously break up, with segmentation of the regions indicated by the red lines. (G) Schematic illustration of a removal event. The point contact between the wrinkle and an AFM tip with a typical radius of 10 nm. Approximately 80% of cut edges show desired shape along the ridges indicated by red lines (i.e., zigzag direction). The cut edges indicated by green curved arrows are not well-defined, and it is unclear which type of edge (i.e., zigzag or armchair edge) is predominant. Reproduced with permission from ref 24. Copyright 2010 American Chemical Society.

Figure 9.[24] Noncontact atomic force microscopy (NC-AFM) images reveal that this structure exhibits a 2D regular arrangement of 1D arrays of epoxy rings running along a zigzag direction. This regular structure can be explained in terms of a 2D arrangement of zigzag-edged graphene nanoribbons with widths of 4.3 nm that are mutually bonded through bridging oxygen atoms (Figure 9G). Previous theoretical analysis[46] supports the formation of the structure illustrated in Figure 9G. Zigzag graphene nanoribbons mutually connected by oxygen bridges can be nanofabricated by cutting with an AFM tip, as illustrated in Figure 9A−F. Manipulation with the AFM tip intentionally creates graphene nanostructures based on zigzag ribbons. Therefore, AFM lithography could be employed to selectively obtain zigzag-edged graphene nanoribbons from graphene oxide, although zigzag edges are thermodynamically unstable due to their lower aromaticity.

8. Concluding Remarks

When a graphene sheet is cut into nanofragments, two distinct edge types, zigzag and armchair, are created. Thus, the electronic structure of the nanographene or graphene edges is significantly dependent on the distinct edge type.

A completely localized nonbonding edge state originates from the broken pseudospin symmetry at the zigzag edges, whereas electron wave interference due to intervalley scattering appears near armchair edge regions. This is a consequence of the singular physical behavior of a massless Dirac fermion in a graphene edge. Chemists understand this in terms of the aromaticity of small PAH molecules. The π radical character of non-Kekulé molecules or open-shell character due to the competition of resonance stabilization between open- and closed-shell forms for the zigzag shaped molecules is strongly reminiscent of the edge state, whereas the fully benzenoid character (in the Clar classification) of armchair shaped molecules is indicative of electron wave interference.

The armchair edges are nonmagnetic and support standing wave states, which are manifested by higher energetic stabilization and lower chemical reactivity. The zigzag edges support strongly localized spin polarized edge states. The edge-state spin plays an important role in the magnetism of nanographene, in contrast to the diamagnetic character of infinite graphene sheets. Moreover, the edge states, which have a large local DOS in the edge region, cause the edge carbon atoms to become chemically active. Nanographene and graphene edges are important topics in physics and chemistry. With the development of bottom-up synthesis and nanofabrication techniques, nanographene and graphene edges will have an important role in future electronics and spintronics device applications.

The authors acknowledge support by Grants-in-Aid for Scientific Research (Nos. 20001006 and 23750150) from MEXT, Japan.

Supporting Information. This material is available free of charge via the Internet at http://pubs.acs.org.

BIOGRAPHICAL INFORMATION

Shintaro Fujii received his Ph.D. in 2005 from the Tokyo Institute of Technology. He was Assistant Professor of the Department of Biomolecular Engineering (2006−2009) and is Research Assistant Professor of the Department of Chemistry (2009 to present) at the Tokyo Institute of Technology.

Toshiaki Enoki received his Ph.D. in 1974 from Kyoto University. He was a Research Associate at the Institute for Molecular Science (1977−1987) and a visiting scientist at the Massachusetts Institute of Technology in 1984. In 1987, he was appointed to the position of Associate Professor of the Department of Chemistry at the Tokyo Institute of Technology, and has since become a Professor. He was a visiting professor at the University of Rennes I (2000, 2004, 2005) and the Institute for Molecular Science (2003−2004), and an honorary professor at Durham University. His current research interests are focused on the magnetic and electronic properties of π-electron-based materials, such as nanographene, nanodiamond, and organic charge transfer complexes.

FOOTNOTES

The authors declare no competing financial interest.

*To whom correspondence should be addressed: E-mail: fujii.s.af@m.titech.ac.jp (S.F.). E-mail: enoki.t.aa@m.titech.ac.jp (E.I.).

REFERENCES

1 Novoselov, K. S.; Geim, A. K.; Morozov, S. V.; Jiang, D.; Zhang, Y.; Dubonos, S. V.; Grigorieva, I. V.; Firsov, A. A. Electric Field Effect in Atomically Thin Carbon Films. *Science* **2004**, *306*, 666–669.

2 Novoselov, K. S.; Jiang, Z.; Zhang, Y.; Morozov, S. V.; Stromer, H. L.; Zeitler, U.; Maan, J. C.; Boebinger, G. S.; Kim, P.; Geim, A. K. Room-Temperature Quantum Hall Effect in Graphene. *Science* **2007**, *315*, 1379.

3 Beenakker, C. W. J. Andreev reflection and Klein tunneling in graphene. *Rev. Mod. Phys.* **2008**, *80*, 1337–1354.

4 Geim, A. K.; Novoselov, K. S. The rise of graphene. *Nat. Mater.* **2007**, *6*, 183–191.

5 Clar, E. *The Aromatic Sextet*; Wiley: London, 1972.

6 Müllen, K.; Rabe, J. P. Nanographenes as Active Components of Single-Molecule Electronics and How a Scanning Tunneling Microscope Puts Them To Work. *Acc. Chem. Res.* **2008**, *41*, 511–520.

7 Niyogi, S.; Hamon, M. A.; Hu, H.; Zhao, B.; Bhowmik, P.; Sen, R.; Itkis, M. E.; Haddon, R. C. Chemistry of Single-Walled Carbon Nanotubes. *Acc. Chem. Res.* **2002**, *35*, 1105–1113.

8 Enoki, T; Kobayashi, Y. Magnetic nanographite: Approach to molecular magnetism. *J. Mater. Chem.* **2005**, *15*, 3999–4002.

9 Loh, K. P.; Bao, Q.; Ang, P. K.; Yang, J. The chemistry of graphene. *J. Mater. Chem.* **2010**, *20*, 2277–2289.

10 Rao, C. N. R.; Sood, A. K.; Subrahmanyam, K. S.; Govindaraj, A. Graphene: The New Two-Dimensional Nanomaterial. *Angew. Chem., Int. Ed.* **2009**, *48*, 7752–7777.

11 Dreyer, D. R.; Park, S.; Bielawski, C. W.; Ruoff, R. S. The chemistry of graphene oxide. *Chem. Soc. Rev.* **2010**, *39*, 228–240.

12 Sinitskii, A.; Tour, J. M. Chemical Approaches to Produce Graphene Oxide and Related Materials. In *Graphene Nanoelectronics: From Materials to Circuits*; Murali, R., Ed.; Springer: New York, 2012; DOI: http://dx.doi.org/10.1007/978-1-4614-0548-1_8.

13 Sakai, K.; Takai, K.; Fukui, K.; Nakanishi, T.; Enoki, T. Honeycomb superperiodic pattern and its fine structure near the armchair edge of graphene observed by low-temperature scanning tunneling microscopy. *Phys. Rev. B* **2010**, *81*, 235417.

14 Sasaki, K.; Wakabayashi, K.; Enoki, T. Berry's phase for standing waves near graphene edge. *New J. Phys.* **2010**, *12*, 083023.

15 Sasaki, K.; Wakabayashi, K.; Enoki, T. Electron Wave Function in Armchair Graphene. *J. Phys. Soc. Jpn.* **2011**, *80*, 044710.

16 Fujii, S.; Enoki, T. Clar aromatic sextet and π electron distribution in nanographene. *Angew. Chem., Int. Ed.* **2012**, *51*, 7236–7241.

17 Fujita, M.; Wakabayashi, K.; Nakada, K.; Kusakabe, K. Peculiar localized state at zigzag graphite edge. *J. Phys. Soc. Jpn.* **1996**, *65*, 1920–1923.

18 Nakada, K.; Fujita, M.; Dresselhaus, G.; Dresselhaus, M. S. Edge state in graphene ribbons: nanometer size effect and edge shape dependence. *Phys. Rev. B* **1996**, *54*, 17954–17961.

19 Kobayashi, Y.; Fukui, K.; Enoki, T.; Kusakabe, K.; Kaburagi, Y. Observation of zigzag and armchair edges of graphite using scanning tunneling microscopy and spectroscopy. *Phys. Rev. B* **2005**, *71*, 193406.

20 Kobayashi, Y.; Fukui, K.; Enoki, T.; Kusakabe, K. Edge state on hydrogen-terminated graphite edges investigated by scanning tunneling microscopy. *Phys. Rev. B* **2006**, *73*, 125415.

21 Enoki, T.; Kobayashi, Y.; Fukui, K. Electronic structures of graphene edges and nanographene. *Int. Rev. Phys. Chem.* **2007**, *26*, 609–645.

22 Niimi, Y.; Matsui, T.; Kambara, H.; Tagami, K.; Tsukada, M.; Fukuyama, H. Scanning tunneling microscopy and spectroscopy studies of graphite edges. *Appl. Surf. Sci.* **2005**, *241*, 43–48.

23 Niimi, Y.; Matsui, T.; Kambara, H.; Tagami, K.; Tsukada, M.; Fukuyama, H. Scanning tunneling microscopy and spectroscopy of the electronic local density of states of graphite surfaces near monoatomic step edges. *Phys. Rev. B* **2006**, *73*, 085421.

24 Fujii., S.; Enoki, T. Cutting of oxidized graphene into nanosized pieces. *J. Am. Chem. Soc.* **2010**, *132*, 10034–10041.

25 Wallace, P. R. The Band Theory of Graphite. *Phys. Rev.* **1947**, *71*, 622–634.

26 Ando, T. Theory of Electronic States and Transport in Carbon Nanotubes. *J. Phys. Soc. Jpn.* **2005**, *74*, 777–817.

27 Krygowski, T. M.; Cyrańsk, M. K. Structural aspect of aromaticity. *Chem. Rev.* **2001**, *101*, 1385–1419.

28 Randić, M. Aromaticity of polycyclic conjugated hydrocarbons. *Chem. Rev.* **2003**, *103*, 3449–3605.

29 Cançado, L. G.; Pimenta, M. A.; Neves, B. R. A.; Medeiros-Ribeiro, G.; Enoki, T.; Kobayashi, Y.; Takai, K.; Fukui, K.; Dresselhaus, M. S.; Saito, R.; Jorio, A. Anisotropy of the Raman spectra of nanographite ribbons. *Phys. Rev. Lett.* **2004**, *93*, 047403.

30 Sasaki, K.; Saito, R.; Wakabayashi, K.; Enoki, T. Identifying the orientation of edge of graphene using G band Raman spectra. *J. Phys. Soc. Jpn.* **2010**, *79*, 044603.

31 Dresselhaus, G.; Dresselhaus, M. S. Spin-Orbit Interaction in Graphite. *Phys. Rev.* **1965**, *140*, A401.

32 Stein, S. E.; Brown, R. L. π-Electron properties of large condensed polyaromatic hydrocarbons. *J. Am. Chem. Soc.* **1987**, *109*, 3721–3729.

33 Stein, S. E. Thermal Reactions and properties of polycyclic aromatic hydrocarbons. *Acc. Chem. Res.* **1991**, *24*, 350–356.

34 Tanaka, K.; Yamashita, S.; Yamabe, H.; Yamabe, T. Electronic properties of one-dimensional graphite family. *Synth. Met.* **1987**, *17*, 143–148.

35 Nakanishi, T.; Ando, T. Conductance between two scanning-tunneling-microscopy probes in carbon nanotubes. *J. Phys. Soc. Jpn.* **2008**, *77*, 024703.

36 Wassmann, T.; Seitsonen, A. P.; Saitta, A. M.; Lazzeri, M.; Mauri, F. Clar's theory, π-electron distribution, and geometry of graphene nanoribbons. *J. Am. Chem. Soc.* **2010**, *132*, 3440–3451.

37 Gutman, I.; Tomović, Ž.; Müllen, K.; Rabe, J. P. On the distribution of π-electrons in large polycyclic aromatic hydrocarbon. *Chem. Phys. Lett.* **2004**, *397*, 412–416.

38 Nakasuji, K.; Kubo, T. Multi-stage amphoteric redox hydrocarbons based on a phenalenyl radical. *Bull. Chem. Soc. Jpn.* **2004**, *77*, 1791–1801.

39 Wassmann, T.; Seitsonen, A. P.; Saitta, A. M.; Lazzeri, M.; Mauri, F. Structure, stability, edge states, and aromaticity of graphene ribbons. *Phys. Rev. Lett.* **2008**, *101*, 096402–1−4.

40 Sasaki, K.; Murakami, S.; Saito, R. Stabilization mechanism of edge states in graphene. *Appl. Phys. Lett.* **2006**, *88*, 113110.

41 Sasaki, K.; Shimomura, Y.; Takane, Y.; Wakabayashi, K. Hamiltonian Decomposition for Bulk and Surface States. *Phys. Rev. Lett.* **2009**, *102*, 146806.

42 Boukhvalov, D. W.; Katsnelson, M. I.; Lichtenstein, A. I. Hydrogen on graphene: Electronic structure, total energy, structural distortions and magnetism from first-principles calculations. *Phys. Rev. B* **2008**, *77*, 035427.

43 Balog, R.; Jørgensen, B.; Wells, J.; Lægsgaard, E.; Hofmann, P.; Besenbacher, F.; Hornekær, L. Atomic Hydrogen Adsorbate Structures on Graphene. *J. Am. Chem. Soc.* **2009**, *131*, 8744–8745.

44 Lomeda, J. R.; Doyle, C. D.; Kosynkin, D. V.; Hwang, W.-F.; Tour, J. M. Diazonium Functionalization of Surfactant-Wrapped Chemically Converted Graphene Sheets. *J. Am. Chem. Soc.* **2008**, *130*, 16201–16206.

45 Bekyarova, E.; Itkis, M. E.; Ramesh, P.; Berger, C.; Sprinkle, M.; de Heer, W. A.; Haddon, R. C. Chemical Modification of Epitaxial Graphene: Spontaneous Grafting of Aryl Groups. *J. Am. Chem. Soc.* **2009**, *131*, 1336–1337.

46 Li, J.-L.; Kudin, K. N.; McAllister, M. J.; Prud'homme, R. K.; Aksay, I. A.; Car, R. Oxygen-driven unzipping of graphitic materials. *Phys. Rev. Lett.* **2006**, *96*, 176101.